Distributions of Epistasis in Microbes Fit Predictions from a Fitness Landscape Model

Guillaume MARTIN[1,2], Santiago F. ELENA[3], Thomas LENORMAND[1]

[1] CEFE-CNRS UMR 5175, 1919 Rte de Mende, 34293 Montpellier, France.

[2] Département d'Ecologie et Evolution, Bâtiment Biophore, Université de Lausanne, 1015 Switzerland. *Present address.*

[3] Instituto de Biología Molecular y Celular de Plantas, Consejo Superior de Investigaciones Científicas-UPV, 46022 València, Spain

Corresponding author: G. Martin

Authors' e-mail
G. Martin: guillaume.martin@unil.ch
S.F. Elena: sfelena@ibmcp.upv.es
T. Lenormand: Thomas.lenormand@cefe.cnrs.fr

running head: mutational epistasis for fitness

How do the fitness effects of several mutations combine? Despite its simplicity, this question is central to our understanding of multilocus evolution. Epistasis —the interaction between alleles at different loci— influences evolutionary predictions[1,2], "almost whenever multilocus genetics matters"[3], in particular epistasis for fitness traits (reproduction, survival). Yet, very few models[4,5] have sought to predict epistasis and none has been empirically tested. Here, we show that the distribution of epistasis can be predicted from the distribution of single mutation effects, based on a simple fitness landscape model[6]. We show that this prediction closely matches the empirical measures of epistasis that have been obtained for the bacterium *Escherichia coli*[7] and the RNA virus VSV[8]. Our results suggest that a simple fitness landscape model may be sufficient to quantitatively capture the complex nature of gene interactions. This model may offer a simple and widely applicable alternative to complex metabolic network models, in particular to include epistasis in evolutionary predictions.

Recent technical improvements in genetics have enabled to measure epistatic interactions in a very precise way. Large amounts of empirical evidence, stemming from the study of development, metabolic networks[5], or quantitative traits analyses[9], have accumulated to show that epistasis is a widespread feature of genetic systems. However, despite numerous examples of epistatic interactions between particular pairs of loci, relatively little is known on the overall distribution of epistasis among random sets of mutations scattered across the genome. A few studies have sought to directly measure this distribution in model systems such as the bacterium *Escherichia coli*[7], RNA viruses[8,10,11], or the brewing yeast *Saccharomyces cerevisiae*[12]. These studies revealed that the variance of epistatic interactions was large compared to their mean, which was always relatively close to zero[10].

Unfortunately, theoretical developments have not gone hand-in-hand with these recent empirical advances and, in particular, no theory is yet available to explain, predict, or generalize these observations. Fitness epistasis among mutations at enzymatic loci has been modeled using Metabolic Control Theory[4] or Flux Balance Analysis (FBA)[5]. The former assumes idealized metabolic pathways and specific metabolism-fitness relationships, whereas the latter models a much more precise and complete metabolic network based on genomic data from model organisms. These approaches propose a clear and valuable mechanistic basis for gene interaction, and FBA has even been successfully tested[13], although only for the extreme case of single gene knockouts. However, FBA requires extensive knowledge of the metabolism of particular organisms in particular environments so it cannot be applied to a wide range of biological systems. Perhaps more importantly, the predicted patterns of epistasis remain to be directly confronted to empirical data.

Despite the relatively minor role that Fisher attributed to epistasis in adaptation, his geometrical model of adaptation[14] provides a general, yet unexplored, framework to predict epistasis among mutations. This model assumes stabilizing selection on n phenotypic traits. The effect of a mutation is modeled as a random displacement in this n-dimensional phenotypic space. Although it has been very useful in rejuvenating the theory of adaptation[15], Fisher's model is often merely viewed as a heuristic picture for mutational effects. However, by avoiding a mechanistic description of the relationship

between particular mutations, phenotypes, and fitness, it allows a global description of mutational effects, without an exhaustive knowledge of the underlying genetic details. This generality is what makes it attractive[16]. In addition, many of the underlying assumptions in Fisher's original model are, in fact, quite realistic[17] or can easily be relaxed[6,18].

Here, we used an extended version of Fisher's geometric model[6], which allows for arbitrary mutational and selective interactions between traits determining fitness (**Fig. 1** illustrates the model and its assumptions). Any model of stabilizing selection (selection for a given optimum) naturally generates epistasis for fitness, even when mutations act additively on the underlying phenotype, because the relationship between phenotype and fitness is non-linear, as illustrated for our particular model on **Figure 1**. The model is formulated in terms of measurable quantities (focusing on mutant fitness W instead of underlying phenotype **z**, **Fig. 1**), which makes it directly comparable to observation. A Gaussian fitness function (relating phenotype to fitness) was chosen because (i) it approximates any smooth function in the vicinity of an optimum and (ii) it qualitatively predicts observed patterns in empirical data, like the gamma distribution of mutational effects in benign environments[6], and the effect of environmental harshness on the mutational mean and variance in fitness[19]. Finally, the model can be easily generalized to describe epistasis among more than two mutations (**Supplementary Methods**).

From this model, three testable predictions were derived (see details and interpretation in Methods). $\text{Log}(w_i)$ denotes the log-fitness of a mutant bearing mutation i, relative to that of the non-mutated initial genotype (eq. (1)). Epistasis among a pair of mutations i and j, e_{ij}, is defined (eq. (2)) as the difference between the log-fitness of the double mutant and that expected if mutations acted multiplicatively: $e_{ij} \equiv \log(w_{ij}) - \log(w_i w_j)$. The model first predicts that the probability density function of e_{ij} is well approximated by a Gaussian with mean zero and variance $2v_s^*$, where $v_s^* = Var(\log(w_i))$ is the variance of single mutation effects measured in an environment to which the initial genotype is well-adapted (eq. (3)). The second prediction of the model is that epistasis among pairs of beneficial mutations should be both biased and skewed towards negative values. Third, the model predicts that when the initial genotype is at or near the optimum, the distribution of log-fitnesses among mutant lines with k mutations (all deleterious) can be approximated by a Gamma distribution $\Gamma(\beta, \alpha)$ with a constant shape (β) and a scale (α) proportional to k.

These three predictions have been tested with data from two widely different species, the bacterium *E. coli*[7] and vesicular stomatitis virus (VSV)[8](see **Fig. 2**). The two first lines of **Table 1** report the tests for the first prediction. For each species three predictions have been tested (eq. (3)): among all pairs of mutations, $E(e_{ij}) = 0$, $Var(e_{ij}) = 2v_s^*$, and $e_{ij} \sim N(0,2v_s^*)$. None of these hypotheses was rejected. As already outlined in the original studies, $E(e_{ij})$ does not significantly depart from 0 in both *E. coli* and VSV. Furthermore, the observed $Var(e_{ij})$ are very close to the predictions (< 5% difference) if synthetic lethals are discarded. Finally, overall, the distributions are not significantly different from the predicted Gaussian $N(0,2v_s^*)$ (**Table 1** and **Fig. 2**). The power curves for these tests (see **Supplementary Fig. 3**) also indicate that even if small departures from the null hypotheses could not be detected, the "true" differences between observations and predictions are likely to be relatively small (except perhaps for the $E(e_{ij})$ value observed for *E. coli*).

The second prediction was tested with the subset of beneficial mutations that were analyzed in the VSV experiments. The model does not provide an analytical expression for the distribution of e_{ij} among beneficial mutations and therefore, the test was performed by confronting the observed epistasis with a simulated distribution, with parameters inferred from the distribution of single mutant fitnesses. **Table 1** summarizes these tests, and **Fig. 3** illustrates the agreement of the empirical and predicted distributions (note that among the subset of beneficial mutations, $E(e_{ij}) < 0$ is expected and observed). None of the predictions regarding the mean, variance, or distribution of e_{ij} were rejected, and the power of these tests was reasonably good (**Supplementary Fig. 3**). However, this comparison has obvious limitations, being based on only 15 double mutants constructed from six distinct beneficial mutations.

Testing the third prediction requires fitting gamma distributions to the log-fitness of mutant lines carrying a known number k of mutations, to check whether the change in shape (β_k) and scale (α_k) with k conforms to the prediction. We used an extensive collection of *E. coli* genotypes differing in the location and number of transposon-insertions[7] (see Methods). This dataset consists in log-fitness measures of genotypes carrying either k = 1, 2, or 3 random insertions, with 75 different combinations per k value. To estimate the log-fitness distributions for each k value, independent gamma distributions were fitted to the data by maximum-likelihood (model 1 of **Table 2**, see Methods), discarding four synthetic lethals. These estimates were compared to alternative data fits where α and/or β are constrained according to k values, following alternative predictions. **Table 2** gives the Akaike's Information Criterion (AIC)[20] for several alternative models, and the parameter estimates for the best-fitting models. The model imposing exactly our theoretical expectation (eq. (A.5) of **Supplementary Methods**: $\beta_k = \beta_1$ and $\alpha_k = k\alpha_1$) is the most adequate one (lowest AIC, model 4). When directly estimated (model 1), the parameters are indeed very close to the model prediction (**Supplementary table** and **Fig. 4**). Thus, the form of epistasis and its impact on log-fitness distributions seems accurately captured by the model.

Overall, the distribution of epistasis for fitness predicted from a simple fitness landscape model adequately accounts for empirical distributions among both pairs and triplets of non-lethal mutations (including between beneficial ones). To our knowledge, this is the first empirical support given for a general model of epistasis. The inherent simplicity in this model allows making testable predictions, which are rarely available at this degree of generality in other models connecting genotype to phenotype to fitness, and offers an alternative to the more complex and specific metabolic network models recently developed[5]. The quantitative accuracy and generality of the predictions, which are independent of the adaptation level, number of traits or phenotypic correlations, could be useful in many evolutionary predictions (e.g., the evolution of sex[21,22]). Finally, the fit between this general model and data from two remarkably different species suggests that the observed empirical patterns may apply to other species as well. In particular, among a set of random mutations, the average epistasis is small (close to zero) with a large variance (twice that of single effects at the optimum), whereas among only beneficial mutations, average epistasis is negative. The generality of these patterns remains an empirical issue, and being fairly quantitative, they are open to further test, especially in higher eukaryotes.

METHODS

Model. Following Lande[23], the fitness $W(\mathbf{z})$ of a phenotype $\mathbf{z}$ (of dimension n, the number of phenotypic traits under selection) is given by a multivariate Gaussian function $W(\mathbf{z}) \equiv \exp(-½\ \mathbf{z}^T\cdot\mathbf{S}\cdot\mathbf{z})$ where ^{T} denotes transposition, and $\mathbf{S}$ is an arbitrary $n\times n$ symmetric positive semi-definite matrix that describes all the selective interactions between phenotypic traits. Note that the fitness function may therefore be flat on some directions of the landscape (if $\mathbf{S}$ has some null eigenvalues). The initial non-mutated genotype's phenotype vector is denoted $\mathbf{z}_o$, and its level of adaptation is measured by $s_o \equiv -\log W(\mathbf{z}_o) = ½\ \mathbf{z}_o^T\cdot\mathbf{S}\cdot\mathbf{z}_o$. The phenotypic effect of a mutation i is given by the vector $\mathbf{dz}_i$, so the mutant phenotype is $\mathbf{z}_o + \mathbf{dz}_i$, and its log-relative fitness is[6]

$$\log(w_i) = \log(W(\mathbf{dz}_i + \mathbf{z}_o)/W(\mathbf{z}_o)) = -\mathbf{z}_o^T\cdot\mathbf{S}\cdot\mathbf{dz}_i - ½\ \mathbf{dz}_i^T\cdot\mathbf{S}\cdot\mathbf{dz}_i. \quad (1)$$

Note that the $\mathbf{dz}_i$ here refers in fact to genotypic values (averaged over replicates of a given line) not to individual replicate phenotypes (which are also influenced by micro-environmental effects). It can be shown (ref. 24 and **Supplementary Note**) that if fitness $W(\mathbf{z})$ is a Gaussian function of individual phenotypes, then log-relative fitness is necessarily a quadratic function of genotypic values as used here, so that environmental effects on phenotype can be ignored. This model has received indirect support from empirical distributions of single mutation effects[6,19]. The effects of mutations on phenotype were assumed additive, so that the joint effect of mutations i and j is $\mathbf{dz}_{ij} = \mathbf{dz}_i + \mathbf{dz}_j$. Importantly, the model is robust to this fairly strong assumption (see **Supplementary Fig. 2**). From eq. (1), if $w_{ij} \equiv W(\mathbf{z}_o + \mathbf{dz}_{ij})/W(\mathbf{z}_o)$ is the relative fitness of the double mutant, then pairwise epistasis, defined as $e_{ij} \equiv \log(w_{ij}) - \log(w_i\ w_j)$, is given by

$$e_{ij} = -\mathbf{dz}_i^T\cdot\mathbf{S}\cdot\mathbf{dz}_j. \quad (2)$$

From eq. (2), it appears that fitness epistasis between two given mutations does not depend on $\mathbf{z}_o$, the position of the wild-type in phenotypic space (i.e. of its degree of adaptation to the environment). This stems from the fact that we assumed a Gaussian fitness function. Indeed, epistasis e_{ij} depends on the curvature of the log-fitness function ($\log W(\mathbf{z})$, see **Fig. 1**), and this curvature is the same for all $\mathbf{z}$ with a quadratic log-fitness (or Gaussian fitness).

To predict the distribution of e_{ij} from eq. (2), assumptions must be made on the distribution of mutation effects on phenotype (the $\mathbf{dz}$). We assume that $\mathbf{dz}$ is drawn into a multivariate Gaussian distribution with mean $\mathbf{0}$ and arbitrary covariance matrix $\mathbf{M}$. Then, e_{ij} is a bilinear form in Gaussian vectors[25] whose moments can be related to those of the distribution of single effects, $\log(w_i)$ given in eq. (1). At the optimum ($s_o = 0$ and $\mathbf{z}_o = \mathbf{0}$ in eq. (1)), the variance v_s^* of $\log(w_i)$ is[6] $v_s^* = Var(-½\ \mathbf{dz}_i^T\cdot\mathbf{S}\cdot\mathbf{dz}_i) = ½\ \mathrm{Tr}((\mathbf{S}\cdot\mathbf{M})^2)$, where $\mathrm{Tr}(\cdot)$ denotes matrix trace. Now, from eq. (2) and because $\mathbf{dz}_i$ and $\mathbf{dz}_j$ are independent ($Cov(\mathbf{dz}_i,\mathbf{dz}_j) = \mathbf{0}$), we find, for e_{ij}, a mean $\mu_e \equiv E(e_{ij}) = E(-\mathbf{dz}_i^T\cdot\mathbf{S}\cdot\mathbf{dz}_j) = 0$ and, because the phenotypic effects $\mathbf{dz}_i$ are multivariate Gaussian, the variance of epistasis is given by

$$v_e \equiv Var(e_{ij}) = Var(-\mathbf{dz}_i^T\cdot\mathbf{S}\cdot\mathbf{dz}_j) = \mathrm{Tr}((\mathbf{S}\cdot\mathbf{M})^2) = 2v_s^*. \quad (3)$$

For the same reasons, the distribution of e_{ij} has also no skewness so that the Gaussian $N(0, 2v_s^*)$ provides a simple and accurate approximation to the distribution of e_{ij} (see **Supplementary Fig. 1.a**), depending on a single parameter (v_s^*). When the initial genotype is *not* at the optimum ($s_o>0$), the variance of $\log(w_i)$ is not equal to v_s^* but must be corrected[6] with a measure of s_o, as $v_s^* \approx Var(\log(w_i))/(1 + 2s_o/\bar{s})$, where $\bar{s} = E(\log(w_i))$ is the mean effect of single mutations on log relative fitness. This correction was used for the VSV dataset.

The prediction $v_e = 2\ v_s^*$ in eq. (3) is fairly general. In particular, as eq. (2) does not depend on $\mathbf{z}_o$, this relation is valid for any distance to the optimum s_o. Similarly, as eq. (3) is valid for any **M** and **S**, it does not depend on the details of the phenotypic landscape: the number of traits n (dimension of **M** and **S**), or their mutational and selective correlations (elements of **M** and **S**). Although these parameters do influence distributions of single mutation fitness effects[6], they do not alter the relationship between single and multiple mutant fitnesses.

Similarly, the distribution of e_{ij} among only beneficial mutations can be obtained for a given fitness landscape (though only by numerical simulations). This landscape is well characterized[6] by an 'effective trait effect' λ_e (that depends on the distribution of the eigenvalues of $\mathbf{S}\cdot\mathbf{M}$) and an 'effective number of dimensions' n_e. The distribution of e_{ij} (eq. (2)) in the original landscape (**S**, **M**) is well approximated by its corresponding distribution in the equivalent landscape, for which $\mathbf{S} = \lambda_e\mathbf{I}_{ne}$ and $\mathbf{M} = \mathbf{I}_{ne}$, where $\mathbf{I}_{ne}$ denotes the identity matrix of dimension n_e. As for single mutation effects[6], the approximation fits the two first moments of the whole distribution of e_{ij} among all mutations, but it is also accurate for the subset of beneficial ones (as shown by simulations on **Supplementary Fig. 1.b**). Since both λ_e and n_e can be estimated from a dataset of single mutation effects[6], e_{ij} among beneficial mutations can be numerically simulated for the same dataset, as was done wit the VSV dataset (see **Fig. 3**).

Epistasis among beneficial mutations tends to be negatively biased in this fitness landscape. This fact stems from the non-linear relationship between phenotype and fitness. In the phenotypic landscape described in **Figure 1**, two beneficial mutations necessarily point to very similar directions (i.e. towards the optimum). However, because the fitness function is concave, there is a diminishing return of W on $\mathbf{z}$, along this direction. Therefore, two steps towards the optimum result in a lower fitness than what would be expected from the addition of the fitness effects of each mutation, which corresponds to negative epistasis. More precisely, consider the expression of e_{ij} as given in eq. (2), but in the equivalent landscape (where $\mathbf{S} = \lambda_e\mathbf{I}_{ne}$). If $\mathbf{dx}_i$ and $\mathbf{dx}_j$ are the vectors of effects of mutations i and j in the equivalent landscape, then from eq. (2), e_{ij} can be written $e_{ij} = -\lambda_e\ \mathbf{dx}_i^T\mathbf{dx}_j$. Therefore, the sign of e_{ij} is the sign of minus the cosine of the angle between $\mathbf{dx}_i$ and $\mathbf{dx}_j$. Because two beneficial mutations tend to point to a similar direction (the optimum), their angle is small so their cosine is positive. For this reason, e_{ij} between beneficial mutations tends to be negatively biased. Furthermore, this bias increases when the distance to the optimum decreases (simulations not shown). This is simply due to the fact that the possible directions of $\mathbf{dz}$ resulting in beneficial mutations are more constrained when closer to the optimum, which results in smaller angle between these mutations, and therefore more negative epistasis.

The model can also easily be extended to lines carrying more than two mutations (see **Supplementary Methods**). When $s_o \approx 0$, the distribution of log-fitnesses among lines carrying k mutations has mean $E(\log(w|k)) = -k\bar{s}$ and variance $Var(\log(w|k)) = k^2 v_s^*$, where $\bar{s}$ and v_s^* are the mean and variance of log-fitnesses among single mutants ($k = 1$), when $s_o = 0$. Using the same approach as in ref. 6, the log-fitness distributions were approximated by a negative gamma matching the two first moments of the exact distribution given above. If we denote α_k and β_k the scale and shape parameters of the gamma approximation for $\log(w|k)$, we then obtain: $\alpha_k = k\alpha_1$ and $\beta_k = \beta_1$. This simple approximation shows good accuracy, as illustrated by simulations in **Supplementary Figure 1.c**. In the absence of epistasis (additive log-fitness effects), the alternative prediction is given by: $\alpha_k = \alpha_1$ and $\beta_k = k\beta_1$ (see **Supplementary Methods**).

All our predictions stem from three *necessary* and *sufficient* assumptions (summarized in **Fig. 1**): (i) a Gaussian fitness function $W(\mathbf{z})$, (ii) additivity of the effects of mutations on phenotype ($\mathbf{z}$) and (iii) Gaussian distribution of these mutation effects with no bias (zero mean). Together, (i) and (ii) lead to eq. (2), while the remaining predictions require also (iii) to be valid, but are fairly robust to the additivity assumption (ii) as shown in **Supplementary Figure 2**. Note also that assumption (iii) is overly restrictive: as the definition of traits is arbitrary, what is in fact needed is that there exist a transformation of 'real' phenotypic traits such that mutational effects on these 'transformed' traits can be approximated by a Gaussian[6].

Data

To test our predictions, we chose the largest available epistasis datasets. However, we discarded studies based on standing genetic variation instead of newly arisen mutations, including a very large study measuring the whole distribution of epistasis in HIV-1[11]. Indeed, the model is meant to describe newly arisen mutations, and its assumptions (e.g. symmetrical phenotypic distributions) may be invalidated by past selection altering the distribution of phenotypes. Several studies have measured (more or less directly) the mean of e_{ij} among random mutations in model species such as *Drosophila melanogaster*[26], yeast[12] or RNA viruses[10]: many found either a small or no departure from our expectation that $E(e_{ij}) = 0$ (reviewed in refs. 3 and 10). However, fewer studies directly measured its distribution by estimating individual epistasis coefficients among individual pairs of random mutations (not only those conferring visible phenotypes), of known effect, and in homozygous or haploid state (to avoid the confounding effect of dominance), which is what is required to fully test the predictions. To our knowledge, the datasets presented below are the only ones doing so, and with enough replicates to ensure that the power of the statistical analyses is not too low (see **Supplementary Fig. 3**).

E. coli dataset 1: This dataset (Fig. 3 of ref. 7) consists of fitness estimates in *E. coli* genotypes bearing one or two transposons (mini-Tn*10*) insertions. Log relative fitness was estimated for the 27 possible pairs constructed from 9 distinct bacterial genotypes bearing a single mini-Tn*10* insert with known fitness effect, yielding a complete set of $\log(w_i)$ and $\log(w_{ij})$ estimates. In this dataset the variance of single fitness effects v_s^* is directly available since the initial genotype was well adapted to the test environment. This initial genotype has indeed evolved for 10,000 generations in this environment[27] and, correspondingly, not a single beneficial mutation was detected among 225 insertions

tested in that same environment[28]. v_s* was therefore directly measured from $Var(\log(w_i))$ among the whole set of single mutants used to produce the double mutants.

E. coli dataset 2: This dataset (Fig. 2 of ref. 7), corresponds to fitness estimates (replicated three times) for genotypes bearing either k = 1, 2 or 3 random mini-Tn*10* inserts, with 75 distinct mutant genotypes per k value, and a corresponding fitness estimate of the non-mutated genotype (replicated 195 times). It is the largest dataset available for the effect of random mutations, in combination or isolated, that we found in the literature. For the same reason as for VSV dataset, we discarded the non-viable genotypes from our analysis (one for $k = 2$ and three for $k = 3$).

VSV dataset: In this dataset, single and double mutants were created on an infectious cDNA by site directed mutagenesis and recovered after transfection of susceptible cells with the mutant plasmids[8]. As discussed in ref. 29, this recombinant virus was not well adapted to the measure environment, resulting in a proportion ($\approx$ 5%) of mutations with beneficial effects (of up to $\log(w_i) = 0.095$), so that $s_o > 0$. s_o was measured by maximum likelihood fitting of a displaced gamma distribution[6] on the distribution of $\log(w_i)$ of the mutations used to construct the double mutants. The resulting estimate of $s_o = 0.11$ (SE = 0.01) was used to infer $v_s^* = Var(\log(w_i))/(1 + 2s_o/\bar{s})$ where $\bar{s} = E(\log(w_i))$ is the mean fitness effect[6] (see above). The estimated shape $\beta = 1.94$ (SE = 0.47) and the scale $\alpha = 0.095$ (SE. = 0.02) of this distribution were used to infer $n_e = 2.5$ and $\lambda_e = 0.06$ (using eqs. 6.a and 6.b of ref. 6), that were needed (along with s_o) to numerically predict the distribution of e_{ij} among beneficial mutations for this dataset. Note that among the 62 double mutants studied, 3 were non viable (synthetic lethals, $w_{ij} = 0$), and were removed from the dataset as the model cannot account for lethal mutations. Note also that in ref. 8, the results are presented separately for pairs of beneficial and deleterious mutations (15 and 44 pairs, respectively, synthetic lethals excluded), whereas the whole set of random mutations (a total of 44 + 15 = 59 pairs) must be used to test the above first prediction (**Fig. 2** and **Table 1**).

Different methods were used in each species to produce mutations (transposons for *E. coli* vs. point mutations for VSV) but reviews of the empirical literature suggest that this should not result in strong differences for mutation effects on phenotype[30] or fitness traits[6]. The present model directly depends on phenotypic effects of mutations, not on their genetic nature, which may explain why it seems to accurately account for both the VSV and *E. coli* datasets.

Statistical analyses. To test the third prediction on VSV dataset 2, three negative gamma distributions were simultaneously adjusted to the relative fitnesses of single, double and triple mutants taking into account the variance in fitness estimated per line (from three independent replicate measures). Measurement error were assumed to be normally distributed, so that the fitness of each mutant j was drawn from $N(\mu_j, \sigma_j)$. It was also assumed that μ_j values were drawn from a negative gamma distribution $\Gamma(\beta_k, \alpha_k)$ where subscript k (= 1, 2, 3) refers to single, double and triple mutants, respectively. On raw data, there is a strong dependence between measurement error and the magnitude of fitness effects (the three repeated fitness measures of strongly deleterious mutants tend to show much larger variance). To account for this strong heteroscedasticity, a linear

dependence of σ on μ_j was assumed. More specifically, σ_i was modelled as $\sigma + a\mu_j$, where a and σ are estimated from the data. Then the likelihood of the data given the parameters (α_1, α_2, α_3, β_1, β_2, β_3, σ, a) was maximized according to the likelihood function given in eq. (A.6) of **Supplementary Methods**. Alternative models were constructed by constraining α_j and β_j values (models 1-5 in Table 2). Models were compared based on their AIC[20] score and/or by likelihood ratio tests. This analysis confirmed the existence of a strong dependency of measurement error on the magnitude of fitness effects (e.g. in model 1, $a = 0.21$, support limits {0.19, 0.25}).

References:

1. Phillips, P., Otto, S.P. & Whitlock, M.C. Beyond the average: the evolutionary importance of gene interactions and variability of epistatic effects. in *Epistasis and the evolutionary process* (eds. Wolf, J.B., Brodie, E.D. & Wade, M.J.) 20-38 (Oxford University press, 2000).

2. Otto, S.P. & Lenormand, T. Resolving the paradox of sex and recombination. *Nature Reviews Genetics* **3**, 252-261 (2002).

3. Michalakis, Y. & Roze, D. Epistasis in RNA viruses. *Science* **306**, 1492-1493 (2004).

4. Szàthmary, E. Do Deleterious Mutations Act Synergistically - Metabolic Control-Theory Provides a Partial Answer. *Genetics* **133**, 127-132 (1993).

5. Segré, D., DeLuna, A., Church, G.M. & Kishony, R. Modular epistasis in yeast metabolism. *Nature Genetics* **37**, 77-83 (2005).

6. Martin, G. & Lenormand, T. A multivariate extension of Fisher's geometrical model and the distribution of mutation fitness effects across species. *Evolution* **60**, 893-907 (2006).

7. Elena, S.F. & Lenski, R.E. Test of synergistic interactions among deleterious mutations in bacteria. *Nature* **390**, 395-398 (1997).

8. Sanjuàn, R., Moya, A. & Elena, S.F. The contribution of epistasis to the architecture of fitness in an RNA virus. *Proceedings of the National Academy of Sciences of the United States of America* **101**, 15376-15379 (2004).

9. Malmberg, R.L. & Mauricio, R. QTL-based evidence for the role of epistasis in evolution. *Genetical Research* **86**, 89-95 (2005).

10. Burch, C.L., Turner, P.E. & Hanley, K.A. Patterns of epistasis in RNA viruses: a review of the evidence from vaccine design. *Journal of Evolutionary Biology* **16**, 1223-1235 (2003).

11. Bonhoeffer, S., Chappey, C., Parkin, N.T., Whitcomb, J.M. & Petropoulos, C.J. Evidence for positive epistasis in HIV-1. *Science* **306**, 1547-1550 (2004).

12. Wloch, D.M., Borts, R.H. & Korona, R. Epistatic interactions of spontaneous mutations in haploid strains of the yeast *Saccharomyces cerevisiae*. *Journal of Evolutionary Biology* **14**, 310-316 (2001).

13. Fong, S.S. & Palsson, B.O. Metabolic gene-deletion strains of Escherichia coli evolve to computationally predicted growth phenotypes. *Nature Genetics* **36**, 1056-1058 (2004).

14. Fisher, R.A. *The genetical theory of natural selection*, (Oxford University Press, Oxford, 1930).

15. Orr, H.A. The genetic theory of adaptation: A brief history. *Nature Reviews Genetics* **6**, 119-127 (2005).

16. Barton, N.H. & Keightley, P.D. Understanding quantitative genetic variation. *Nature Reviews Genetics* **3**, 11-21 (2002).

17. Orr, H.A. The "sizes" of mutations fixed in phenotypic evolution: a response to Clarke and Arthur. *Evolution & Development* **3**, 121-123 (2001).

18. Waxman, D. & Welch, J.J. Fisher's microscope and Haldane's ellipse. *American Naturalist* **166**, 447-457 (2005).

19. Martin, G. & Lenormand, T. The fitness effect of mutations in stressful environments: a survey in the light of fitness landscape models. *Evolution* (*in press*).

20. Akaike, H. A new look at the statistical model identification. *IEEE Transactions on Automatic Control* **19**, 716-723 (1974).

21. Otto, S.P. & Feldman, M.W. Deleterious mutations, variable epistatic interactions and the evolution of recombination. *Theoretical Population Biology* **51**, 134-147 (1997).

22. Kouyos, R.D., Otto, S.P. & Bonhoeffer, S. Effect of varying epistasis on the evolution of recombination. *Genetics* **173**, 589-597 (2006).

23. Lande, R. The Genetic Covariance between Characters Maintained by Pleiotropic Mutations. *Genetics* **94**, 203-215 (1980).

24. Burger, R. Chapter V 1.2. in *The mathematical theory of selection, recombination, mutation* pp 158 - 160 (John Wiley & Sons Ltd, Chichester, UK, 2000).

25. Mathai, A.M. & Provost, S.B. *Quadratic forms in random variables*, (Marcel Dekker, New York, 1992).

26. Whitlock, M.C. & Bourguet, D. Factors affecting the genetic load in Drosophila: Synergistic epistasis and correlations among fitness components. *Evolution* **54**, 1654-1660 (2000).

27. Lenski, R.E. & Travisano, M. Dynamics of Adaptation and Diversification - a 10,000-Generation Experiment with Bacterial-Populations. *Proceedings of the National Academy of Sciences of the United States of America* **91**, 6808-6814 (1994).

28. Elena, S.F., Ekunwe, L., Hajela, N., Oden, S.A. & Lenski, R.E. Distribution of fitness effects caused by random insertion mutations in *Escherichia coli*. *Genetica* **103**, 349-358 (1998).

29. Sanjuàn, R., Moya, A. & Elena, S.F. The distribution of fitness effects caused by single-nucleotide substitutions in an RNA virus. *Proceedings of the National Academy of Sciences of the United States of America* **101**, 8396-8401 (2004).

30. Kidwell, M.G. & Lisch, D. Transposable elements as sources of variation in animals and plants. *Proceedings of the National Academy of Sciences of the United States of America* **94**, 7704-7711 (1997).

Acknowledgments

We thank D. Waxman and P. Jarne for helpful comments on this work. This work was supported by an Action Concertée Incitative from the French Ministry of Research to T.L. and G.M. benefited from a PhD fellowship from the French Ministry of Research and a grant 31-108194/1 from the Swiss National Science Foundation to J. Goudet. S.F.E. was supported by grant BMC2003-00066 from the Spanish MEC-FEDER.

Figure Legends

Figure 1 Fitness landscape model of epistasis between mutations, based on three main assumptions (listed on the left (i), (ii) and (iii)). An example of the fitness landscape is given with only two phenotypic traits determining fitness, and two mutations *i* and *j* (both beneficial here). Fitness $W(\mathbf{z})$ decreases as a multivariate Gaussian function of the distance to the optimum on both traits, with arbitrary interactions between traits (assumption (i)). From an arbitrary initial phenotype ($\mathbf{z}_o$), distinct mutations (at different loci) produce random perturbations of phenotypic traits ($\mathbf{dz}_i$,$\mathbf{dz}_j$), which act additively on phenotype when combined together ($\mathbf{dz}_{ij}$) (assumption (ii)). Although mutation effects on $\mathbf{z}$ are additive, epistasis measured on log relative fitness (e_{ij}) is naturally generated by the non-linear mapping from phenotype $\mathbf{z}$ to fitness $W(\mathbf{z})$. With stabilizing selection, the curvature of $W(\mathbf{z})$ produces a diminishing return of fitness on phenotype, so that two mutations which effects add up for phenotype, do not add up for fitness (here, the outcome is negative e_{ij}). The more precise quantitative predictions regarding e_{ij} distributions depend on the type of distribution chosen for the $\mathbf{dz}_i$: in our model, a multivariate Gaussian with arbitrary mutational covariances (assumption (iii)).

Figure 2 Observed and predicted distributions of fitness epistasis between random pairs of mutations. The observed distribution of epistasis for log-fitness is presented for two model species (*E. coli* dataset [1][7] and VSV dataset[8]), together with the predicted Gaussian distribution $N(0, 2v_s^*)$, where v_s^* is the variance of single fitness effects (at the optimum, $s_o = 0$) estimated directly (*E. coli*) or inferred (VSV, using the correction for $s_o \neq 0$, see Methods). As an illustration, the dashed line gives the kernel density estimate of the data (a smoothed equivalent of a histogram) with a Gaussian smoothing kernel. The model and data are in very good agreement in both species.

Figure 3 Observed and predicted distributions of epistasis between VSV beneficial mutations[8] (15 epistasis estimates). The predicted distribution (continuous line) is obtained by simulations calibrated with the estimates of n_e, s_o, and λ_e from single mutant log-fitnesses (see Methods and **Table 1**): 1500 mutant phenotypic effect vectors, $\mathbf{dx}_i$, were drawn into a *standard* multivariate Gaussian of dimension $n = n_e = 3$ which is the closest integer to $n_e = 2.5$ estimated from the VSV data. A vector of the multivariate distance to the optimum, $\mathbf{x}_o$, was drawn into the same distribution and scaled so that $-\frac{1}{2}\lambda_e \log(\mathbf{x}_o^T \cdot \mathbf{x}_o) = s_o$ (with $s_o = 0.11$ and $\lambda_e = 0.06$, from the data). The epistasis coefficient between pairs of mutations (i,j) is computed as $e_{ij} = -\lambda_e \mathbf{dx}_i^T \cdot \mathbf{dx}_j$, and we only kept the subset of simulated mutants with beneficial single effect (i.e. $\mathbf{dx}_i$ such that $\log(w_i) = -\lambda_e(\mathbf{x}_o^T \cdot \mathbf{dx}_i + \frac{1}{2}\mathbf{dx}_i^T \cdot \mathbf{dx}_i) > 0$), the resulting distribution is that of e_{ij} among all possible pairs of beneficial mutations for this simulation. This was repeated 20 times to account for the effect of variation of the direction of $\mathbf{x}_o$ for a given s_o. The predicted distribution (plain line), obtained by the overall distribution of e_{ij} among the 20 replicated simulations, is close to the empirical distribution (histogram).

Figure 4 Observed and predicted change of the distribution of log-fitness with the number of mini-Tn*10* insertions in *E. coli*: gamma approximation. Parameters of a

gamma distribution (its rate $1/\alpha$ on panel **a.**, and its shape β on panel **b.**) estimated by maximum likelihood on *E. coli* dataset 2[7], for each subset of mutants (single, double and triple). The estimated values where obtained by independently fitting gamma distributions on each subset (model 1, **Table 2**). The predicted values where obtained by constraining the parameters of the gamma across subsets to follow our prediction (model 4, **Table 2**): α proportional to the number of mutations per line in each subset (one, two or three), and constant β across subsets. Bars give the support limits for the estimates (given in **Supplementary Table**). The unconstrained fit is not significantly better than the fit imposing our prediction (model 4 vs. model 1, $\chi^2 = 2.32$, 4 d.f., $P = 0.68$).

Tables

Table 1 Pairwise epistasis in VSV and *E. coli*: fit to predictions

Species [ref.] (nb. of obs.)	Input parameters (nb. of obs.)	**Epistasis variance** $v_{e\ obs}$ (SE) $v_{e\ pred}$ (SE)	$v_{e\ obs}$ / $v_{e\ pred}$ *F*-test	**Epistasis mean** $\mu_{e\ obs}$ (SE) *t*-test	KS test
E. coli[7] ($n = 27$) (all mutations)	v_s* = 0.033 ($n = 54$)	$v_{e\ obs} = 0.0652$ (0.017) $v_{e\ pred} = 0.0670$ (0.013)	$F_{26,53}$= **97%** $P = 0.94$	$\mu_{e\ obs} = -0.033$ (0.05) $\mu_{e\ pred} = 0$ $t_{26} = -0.66$, $P = 0.51$	$D = 0.18$ $P = 0.30$
VSV[8] ($n = 59$) (all mutations)	v_s* = 0.0047 $s_o = 0.11$[a] ($n = 118$)	$v_{e\ obs} = 0.0089$ (0.0016) $v_{e\ pred} = 0.0094$ (0.0012)	$F_{58,117}$ = **95%** $P = 0.86$	$\mu_{e\ obs} = 0.004$ (0.012) $\mu_{e\ pred} = 0$ $t_{58} = 0.31$, $P = 0.75$	$D = 0.085$ $P = 0.76$
VSV[8] ($n = 15$) (beneficial mutations)	$n_e = 3$[a] $\lambda_e = 0.06$[a] $s_o = 0.11$[a] ($n = 118$)	$v_{e\ obs} = 0.0043$ (0.0016) $v_{e\ pred} = 0.0045$ (.)	$^{obs}/_{pred}$ = **96%** $\chi^2_{14} = 13.4$ $P = 0.99$	$\mu_{e\ obs} = -0.075$ (0.023) $\mu_{e\ pred} = -0.059$ $t_9 = -0.95$, $P = 0.36$	$D = 0.27$ $P = 0.22$

[a] estimates from the fit of the VSV dataset (displaced gamma), with $n = n_e = 3$ in simulations (**Fig.3**) closest integer to the estimated $n_e = 2.5$.

Test of the fit to predictions: observed ($v_{e\ obs}$) and predicted ($v_{e\ pred}$) variances were compared with two-tailed *F*-tests, as the prediction ($v_{e\ pred} = 2v_s$*) is itself based on an independent estimate of v_s*. For beneficial mutations in VSV (third line), the simulated prediction (see Methods) was considered exact (a conservative approach), so that a two-tailed χ^2 test was used. Observed ($\mu_{e\ obs}$) and predicted ($\mu_{e\ pred}$) means were compared using two-tailed *t*-tests. Distributions were not significantly different from a Gaussian (Shapiro-Wilks test: $p = 0.45$ (*E. coli*), $p = 0.44$ (VSV, all mutations), $p = 0.59$ (VSV, beneficial mutations). The predicted and observed overall distributions were also

compared using Kolmogorov-Smirnov (KS) tests (one sample tests with $N(0, 2v_s^*)$, or two sample test with the simulated prediction for beneficial mutations in VSV). The second column gives the value of the input parameters used in the prediction, estimated independently from the log-fitness distributions of the single mutants from which the double mutants were derived. None of the observed distributions differ significantly from the predictions. The ratios of variances (in bold) show that the prediction is always within 5% of the estimation. Power curves for the *t* and *F*-tests are illustrated on **Supplementary Figure 3**.

Table 2 Effect of the number of mutations in *E. coli*: model comparison.

Model	Constraints	*df*	*Dev*	*AIC*
1 [a]	$\alpha_1, \alpha_2, \alpha_3 \mid \beta_1, \beta_2, \beta_3$	8	0	16
2	$\alpha_1, \alpha_2, \alpha_3 \mid \beta_1 = \beta_2 = \beta_3$	6	0.08	12.08
3	$\alpha_1 = \alpha_2 = \alpha_3 \mid \beta_1, \beta_2, \beta_3$	6	8.24	20.24
4 [b]	$\alpha_2 = 2\alpha_1, \alpha_3 = 3\alpha_1 \mid \beta_1 = \beta_2 = \beta_3,$	4	2.32	**10.32**
5	$\alpha_1 = \alpha_2 = \alpha_3 \mid \beta_1 = \beta_2 = \beta_3$	4	21.8	29.8

[a] estimate: shape β and scale α fitted independently for each mutant subsets.
[b] our prediction: constant shape β and increasing scale $\alpha_k = k\alpha_1$.

Models fitted for *E. coli* dataset 2^7. β_k and α_k refer to the shape and scale of the gamma distributions fitted to the log-fitness distributions of distinct mutant sets (carrying $k = 1$, 2 or 3 mini-Tn*10* insertions). Models are spelled out by the constraints imposed among these parameters in the fitting process. For each model are indicated, the number of fitted parameters (*df*), the residual deviance (*Dev*) and the Akaike Information Criterion *(AIC)*. Model 1 is unconstrained and provides the direct *estimation* of β_k and α_k, the distributions for $k = 1$, 2 or 3 are fitted independently. Its fit is not significantly better ($\chi^2 = 2.32$, 4 d.f., $P = 0.68$) than that of Model 4 (more constrained) which corresponds to our prediction (constant shape β and increasing scale $\alpha_k = k\alpha_1$, see **Supplementary Methods**) and which is the most adequate model (lowest *AIC*). Similarly, model 2 (constraining shapes to be identical) is not significantly better than model 4 ($\chi^2 = 2.24$, 2 d.f., $P = 0.33$). Model 3 corresponding to multiplicative fitness effects ($e_{ij} = 0$, see **Supplementary Methods**) and model 5 (all distributions equal) are both rejected, showing that the analysis has enough statistical power to reject inaccurate models.

Supplementary Methods: epistasis in genotypes bearing more than two mutations

I) Distribution of log-fitness with an arbitrary number of mutations

In this appendix, we compute the mean $E(\log(w|k))$ and variance $Var(\log(w|k))$ of the log relative fitness among lines carrying exactly k mutations. Denote $\{\mathbf{dz}_i\}_{i\in[1,k]}$, the set of vectors describing the effect of each of the k mutations on phenotype. Assuming that mutations act additively on phenotypic traits, the resulting mutant phenotype is the sum of each effect: $\mathbf{z} = \mathbf{z}_o + \sum_{i=1}^{k} \mathbf{dz}_i$. Under the Gaussian fitness function assumed in our model, the log-fitness of this mutant is $\log(W(\mathbf{z})) = -\frac{1}{2}\, \mathbf{z}^T \cdot \mathbf{S} \cdot \mathbf{z}$ where ^{T} denotes transposition. Then, the log-relative fitness of the mutant ($\log(W(\mathbf{z})/W(\mathbf{z}_o))$ carrying the k mutations with effects $\{\mathbf{dz}_i\}_{i\in[1,k]}$ is then given by:

$$\begin{aligned} \log(w(\mathbf{z})) &= \log\left(W\left(\mathbf{z}_o + \sum_{i=1}^{k} \mathbf{dz}_i\right)\right) - \log\left(W(\mathbf{z}_o)\right) \\ &= \sum_{i=1}^{k} s_i - \sum_{i=1}^{k}\sum_{j=i+1}^{k} \mathbf{dz}_i^T . \mathbf{S} . \mathbf{dz}_j \end{aligned}, \qquad (A.1)$$

where $s_i = \log(w_i) = -\mathbf{z}_o^T \cdot \mathbf{S} \cdot \mathbf{dz}_i - \frac{1}{2}\, \mathbf{dz}_i^T \cdot \mathbf{S} \cdot \mathbf{dz}_i$ is the single log-fitness effect of mutation i (see Methods), denoted s_i below. Rewriting (A.1) with our definition of epistasis based on log-fitness, $e_{ij} = -\mathbf{dz}_i^T \cdot \mathbf{S} \cdot \mathbf{dz}_j$, we get the relative fitness of a mutant bearing k mutations with individual effects $\{s_i\}_{i\in[1,k]}$:

$$\log(w|k) = \sum_{i=1}^{k} s_i + \sum_{i=1}^{k}\sum_{j=i+1}^{k} e_{ij} . \qquad (A.2)$$

Therefore, with a Gaussian fitness function and additive mutation effects on phenotype, there is no epistasis of order higher than two (e_{ijk}). In addition, because the $\mathbf{dz}_i$ are *independently* drawn into a multivariate Gaussian distribution, for any $i \neq j$ $Cov(\mathbf{dz}_i, \mathbf{dz}_j) = 0$, so that there are no covariances between the terms in the sums in (A.2). Indeed, under these assumptions, $Cov(\mathbf{dz}_i, \mathbf{dz}_{i'}^T \cdot \mathbf{S} \cdot \mathbf{dz}_{j'}) = 0$ and $Cov(\mathbf{dz}_i^T \cdot \mathbf{S} \cdot \mathbf{dz}_j\, , \mathbf{dz}_i^T \cdot \mathbf{S} \cdot \mathbf{dz}_{j'}) = 0$ for any pair $\{i,j\} \neq \{i',j'\}$. This implies that $Cov(s_i, s_j) = Cov(s_i, e_{i'j'}) = Cov(e_{ij}, e_{i'j'}) = 0$. Because of this independence, we can apply the expectation and variance operators on each term of the sums in (A.2). Define $\bar{s} = -E(s_i)$, the average log-fitness effect of single mutations, $v_s = Var(s_i)$ their variance, and $v_e = Var(e_{ij})$ the variance of epistasis among random pairs of mutations. Then, using (A.2) and the fact that the average epistasis is zero ($E(e_{ij}) = 0$) gives the mean and variance of $\log(w|k)$,

$$\begin{aligned} E\left(\log(w|k)\right) &= -k\, \bar{s} \\ Var\left(\log(w|k)\right) &= k\, v_s + \frac{k(k-1)}{2} v_e \end{aligned} . \qquad (A.3)$$

Furthermore, if the initial phenotype is well adapted to the environment where fitness is measured ($s_o \approx 0$), then $v_s = v_s^*$ by definition, and as we have shown that $v_e = 2v_s^*$ (see Methods), (A.3) simplifies to

$$E\left(\log\left(w\,|\,k\right)\right) = -k\,\bar{s} \text{ and } Var\left(\log\left(w\,|\,k\right)\right) = k^2 v_s^*. \quad \text{(A.4)}$$

Matching these exact moments to those of a negative gamma distribution with scale and shape α_k and β_k, gives $E(\log(w|k)) = -\alpha_k \beta_k$, $Var(\log(w|k)) = \alpha_k^2 \beta_k$, which, by identification with (A.4) gives

$$\alpha_k = k\,\frac{v_s^*}{\bar{s}} = k\,\alpha_1 \text{ and } \beta_k = \frac{\bar{s}^2}{v_s^*} = \beta_1 \quad \text{(A.5)}$$

From that, it is straightforward to derive the simple relationships between the rate parameter ($1/\alpha_k$), the shape (β_k) and k used to fit the *E. coli* dataset 2 (**Fig. 4** and model 4 of **Table 2** and **Supplementary table**). Conversely, when epistasis is neglected, $v_e = 0$ in (A.3), so that $E(\log(w|k)) = k\bar{s}$ and $Var(\log(w|k)) = k\,v_s^*$, yielding another relationship between k and the parameters: $\alpha_k = \frac{v_s^*}{\bar{s}}$ and $\beta_k = k\frac{\bar{s}^2}{v_s^*}$. This relationship was used for model 3 of **Table 2** but with less constraint: a constant α was fitted across mutant subsets (k = 1, 2, 3), while β was estimated independently for each k value. The exact constrained model (i.e. β increasing linearly with k) is even worse, and was not implemented.

II) Maximum-likelihood analysis of the fitness distribution of single, double and triple mutants

The log-likelihood of the log relative fitnesses (**w**) of single, double and triple mutants on VSV dataset 2 was computed as

$$\ln \Pr\left(\mathbf{w}|\boldsymbol{\beta},\boldsymbol{\alpha},\sigma,a\right) = \sum_{k=1}^{3}\sum_{j} \ln\left(\int_{\mu=0}^{\infty} \Gamma(\beta_k,\alpha_k;\mu)\prod_i N(\mu,\sigma+a\mu;-w_{ijk})\,d\mu\right) \quad \text{(A.6)}$$

where $\Gamma(\beta,\alpha;x)$ and $N(\mu,\sigma;x)$ denote the probability density function of the Gamma distribution (with shape β and scale α) and of the Normal distribution with mean μ and standard deviation σ (increasing linearly with the mean: coefficient a), respectively. The log-relative fitness of a mutant line ($\log(W(\mathbf{z})/W(\mathbf{z}_o))$ is noted w_{ijk} (note the minus sign snext to w_{ijk} because log-fitness is negative and the gamma is positive). Index k refers to simple, double and triple mutants (k = 1, 2, 3), index j to the mutant lines and index i to the repeated fitness measures for a given line j. Vectors $\boldsymbol{\beta} = \{\beta_k\}_{k\in[1,3]}$ and $\boldsymbol{\alpha} = \{\alpha_k\}_{k\in[1,3]}$ refer to the parameters of the gamma distribution for each mutant subset.

For the estimation of the parameters (model 1 in Table 2), each parameter (α_1, β_1, α_2, β_2, α_3, β_3, μ, a) were fitted independently. For the alternative models (2-5), distinct constraints (detailed in Table 2) were imposed on α and β as a function of k.

Supplementary Note: Fitness as a function of phenotypes *vs.* of genotypic values

At first glance, our model ignores the environmental variance on phenotypes and its impact on fitness estimation. Yet, some micro-environmental effects among replicates of the same line should alter the phenotypes **z**, and in turn introduce a bias in the log fitnesses log*W*. In quantitative genetics (see e.g. ref. 1), this problem is overcome by defining the fitness function not in terms of phenotypes **z** but in terms of genotypic values. Following this approach, vector $\mathbf{z}_i = \mathbf{z}_o + \mathbf{dz}_i$ in our model represents the genotypic value of a mutant line *i* (with mutation phenotypic effect $\mathbf{dz}_i$), which is an average over replicated fitness measures of mutant line *i* (like in the datasets we used). We show below that provided environmental effects are independent of genotypes, the assumptions of a Gaussian fitness function of phenotype and of genotypic values are equivalent in terms of the log-fitness functions log*W*(.).

If we denote by vector $\mathbf{p}_{ij}$ the phenotype of the j^{th} replicate of line *i* then this phenotype is the sum of the genotypic value of line *i* ($\mathbf{z}_i$) plus a contribution of the environment for this particular replicate *j* (vector $\boldsymbol{\xi}_{ij}$). We assume, as is usual[1], that this contribution is independent of the genotype (i.e. of $\mathbf{z}_i$) and multivariate Gaussian with mean vector **0** and arbitrary covariance matrix $\mathbf{V}_e$. We first write fitness *W*(.) as a Gaussian function of phenotype

$$W(\mathbf{p}_{ij}) = exp\left(-\frac{1}{2}\mathbf{p}_{ij}{}^{\mathrm{T}}\mathbf{W}^{-1}\mathbf{p}_{ij}\right), \qquad \text{(B.1)}$$

where **W** is a symmetric positive-definite matrix. In this case, by taking the expectation of *W* over the distribution of environmental effects $\boldsymbol{\xi}_{ij}$ for a given genotype $\mathbf{z}_i$, it can be shown[1] that fitness *W* is also a Gaussian function of genotypic values **z**,

$$W(\mathbf{z}_i) = exp\left(-\frac{1}{2}\mathbf{z}_i{}^{\mathrm{T}}\mathbf{V}_s{}^{-1}\mathbf{z}_i\right), \qquad \text{(B.2)}$$

where $\mathbf{V}_s = \mathbf{W} + \mathbf{V}_e$. Therefore, as long as the fitness values used are averaged over several replicates per lines (which is our case) we can use a Gaussian fitness function directly on genotypic values **z**, thus getting rid of the effect of the environment.

The argument is still valid in the more general case (assumed in this paper) of semi-definite matrices, for which $\mathbf{W}^{-1}$ in (B.1) may not exist. However, it is so only when considering log-relative fitness functions (as we do here), not absolute fitness. Let us consider our general fitness function replacing $\mathbf{W}^{-1}$ by **S** in (B.1), for the phenotype – fitness function, and assuming **S** is only semi-definite. Using the fact that $\mathbf{p}_{ij} = \mathbf{z}_i + \boldsymbol{\xi}_{ij}$, we can express the log fitness of the j^{th} replicate of genotype *i* as

$$\log W(\mathbf{p}_{ij} = \mathbf{z}_i + \boldsymbol{\xi}_{ij}) = -\frac{\mathbf{z}_i{}^{\mathrm{T}}\mathbf{S}\,\mathbf{z}_i}{2} + \frac{\boldsymbol{\xi}_{ij}{}^{\mathrm{T}}\mathbf{S}\,\boldsymbol{\xi}_{ij}}{2} + \mathbf{z}_i{}^{\mathrm{T}}\mathbf{S}\,\boldsymbol{\xi}_{ij}\,. \qquad \text{(B.3)}$$

Like for (B.2), we can express the fitness function in terms of genotypic instead of phenotypic values by taking the expectation of log$W$ over the distribution of environmental effects $\boldsymbol{\xi}_{ij}$ for a given genotype $\mathbf{z}_i$, which gives

$$\begin{aligned}\log W(\mathbf{z}_i) = E\left(\log W \mid \mathbf{z}_i\right) &= -\frac{\mathbf{z}_i{}^{\mathrm{T}}\mathbf{S}\,\mathbf{z}_i}{2} - E\left(\frac{\boldsymbol{\xi}_{ij}{}^{\mathrm{T}}\mathbf{S}\,\boldsymbol{\xi}_{ij}}{2}\right) - \mathbf{z}_i{}^{\mathrm{T}}\mathbf{S}\,E(\boldsymbol{\xi}_{ij}) \\ &= -\frac{\mathbf{z}_i{}^{\mathrm{T}}\mathbf{S}\,\mathbf{z}_i}{2} - \frac{1}{2}Tr(\mathbf{S}.\mathbf{V}_{\mathrm{e}})\end{aligned}, \qquad \text{(B.4)}$$

where $Tr(.)$ denotes matrix trace (recall that $E(\boldsymbol{\xi}_{ij}) = \mathbf{0}$). Therefore we also retrieve a log-quadratic function, modulo a constant: $-\frac{1}{2}\,\mathrm{Tr}(\mathbf{S}.\mathbf{V}_e)$ in (B.4). When we consider the log-relative fitness (as done in our model): $\log(W(\mathbf{z}) / W(\mathbf{z}_o)) = \log W(\mathbf{z}) - \log W(\mathbf{z}_o)$, the constant in (B.4) disappears, since it contributes to the log fitness of both the wild-type ($\mathbf{z}_o$) and the mutant ($\mathbf{z}$). Then, using $\mathbf{z}_i = \mathbf{z}_o + \mathbf{d}\mathbf{z}_i$, we retrieve eq. (1) (main text) for the log-relative fitness of mutant i. Note that, as E(log$W$) in (B.4) is slightly different from log(E(W)) as derived from (B.2), the equivalence between quadratic log-fitness for phenotype and for genotypic values is only approximate (with weak selection coefficients), when $\mathbf{S}$ is only semi-definite, while it is exact when $\mathbf{S}$ is definite.

References:

1. Burger, R. Chapter V 1.2. in *The mathematical theory of selection, recombination, mutation* pp 158 - 160 (John Wiley & Sons Ltd, Chichester, UK, 2000).

Supplementary table: Parameter estimation for the MCMC fit

ML Estimates	$E(1/\alpha)$			$E(\beta)$		
number of mutations *k*	1	2	3	1	2	3
model 1	40.7	16.8	16.1	0.76	0.71	0.76
support limits (2 log *L*)	(30.2 – 50.9)	(12.5 - 22.1)	(12.0 – 21.1)	(0.59 - 0.94)	(0.57 - 0.87)	(0.61 - 0.92)
model 4	39.2	19.6	13.1	0.73	0.73	0.73
support limits (2 log *L*)	(33.1 - 46.0)	n/a	n/a	(0.63 - 0.82)	(0.63 - 0.82)	(0.63 - 0.82)
model 4 / model 1	**96%**	**117%**	**81%**	**96%**	**103%**	**96%**

Maximum likelihood (ML) estimates of the parameters of the gamma distributions $\Gamma(\beta, \alpha)$ describing the fitness of *E. coli* genotypes with k = 1, 2 or 3 mini-Tn*10* insertions[7] (see also **Table 2** and **Fig. 4**). $1/\alpha$ is the rate parameter (1/scale) and β is the shape parameter of the Gamma distribution. The estimates are given for model 1 (distributions fitted independently for each k values) and model 4 which constrains for a constant shape and a scale α proportional to k (or rate proportional to $1/k$, our prediction). Support limits correspond to the region within 2 units of log-likelihood from the maximum. The ratios of estimates between model 1 and 4 (expressed in %) are all close to one, showing the good agreement between the unconstrained fit (model 1, estimate of the parameters) and the model constrained to follow our prediction (model 4).

Supplementary Figure 1: agreement of the predicted approximate distributions with simulations

a) Pairwise epistasis: Gaussian approximation

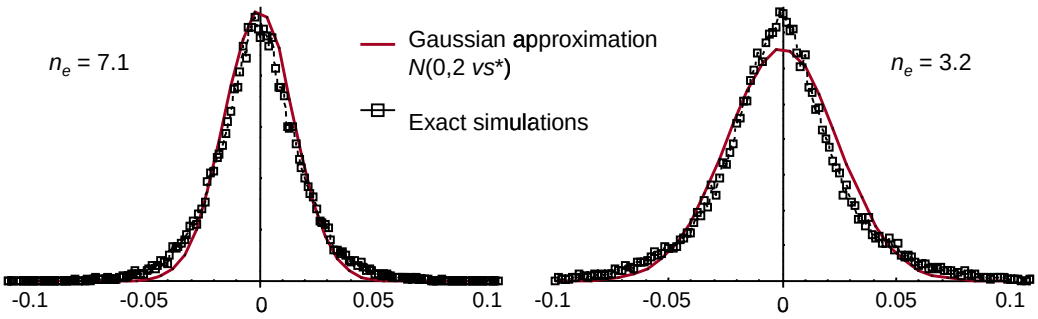

Epistasis between random mutations e_{ij}

b) Pairwise epistasis among beneficial mutations: Equivalent landscape approximation

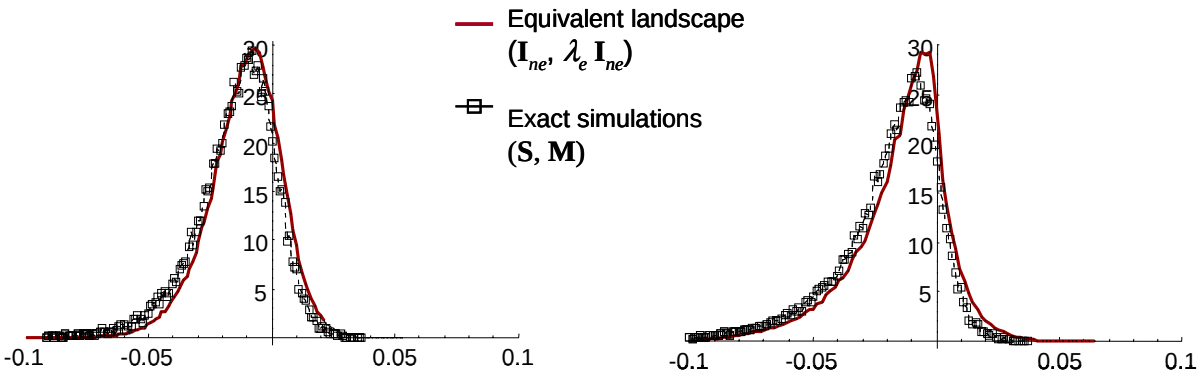

Epistasis between beneficial mutations e_{ij}

c) Distribution of log-fitness for *k* mutations: gamma approximation

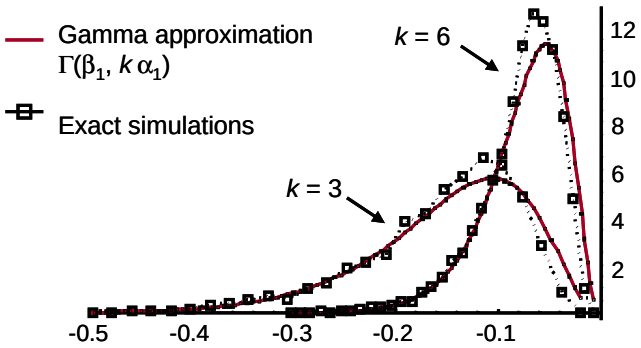

Mutant log relative fitness with *k* mutations

a)
The distribution of $e_{ij} = \log(w_{ij}) - \log(w_i\, w_j)$ is simulated by drawing 5000 vectors of mutation effects ($\mathbf{dz}_i$) into a multivariate Gaussian of dimensions n = 100 phenotypic traits, with strongly heterogeneous effects for both mutation and selection following the method in ref. 6. The selective and mutational covariance matrices are drawn randomly from a Wishart distribution (a classic null model of covariance matrix[6]), and scaled so that the average effect of single mutations is $\overline{s} = 0.025$. The resulting effective number of dimensions n_e is strongly reduced (indicated on the figure). The initial phenotype from which mutations arise is not perfectly adapted: a vector $\mathbf{z}_o$ is drawn into a multivariate Gaussian so that $s_o = 0.07$.

The figure shows that, even away from the optimum (s_o>0), the agreement between simulations and the approximation of the pdf by a centered Gaussian $N(0,2v_s^*)$ is always fairly good, although it can be significantly lessened for very small n_e values (right panel).

b)
Same as **a)** (right and left panels) but focusing only on epistasis between beneficial mutations. In this case we have no analytic prediction, but only the distribution obtained by simulations of the equivalent landscape (red line). Simulations of the equivalent landscape were repeated by drawing several vectors of the distance to the optimum $\mathbf{x}_o$ with the same s_o (as for the VSV data in **Figure 3**). This allows to average-up the effect of the direction of $\mathbf{x}_o$ in the landscape (for a given distance s_o).

c)
The distribution of log-fitness for mutants carrying k mutations is shown for k = 3 and 6. Each single mutation's effect vector $\mathbf{dz}_i$ is simulated as in **Supplementary Figure 1. a.**, except that s_o = 0, and a given mutant carries k such mutations with additive effects on phenotype, resulting in a single phenotypic vector $\mathbf{dz} = \sum_{i=1}^{k} \mathbf{dz}_i$.

The figure shows that the gamma approximation given in **Supplementary Methods** and used to fit the *E. coli* dataset 2 (**Figure 4**) is in good agreement with exact simulations.

Supplementary Figure 2: Robustness of the model to non-additivity in the phenotypic effects of mutations.

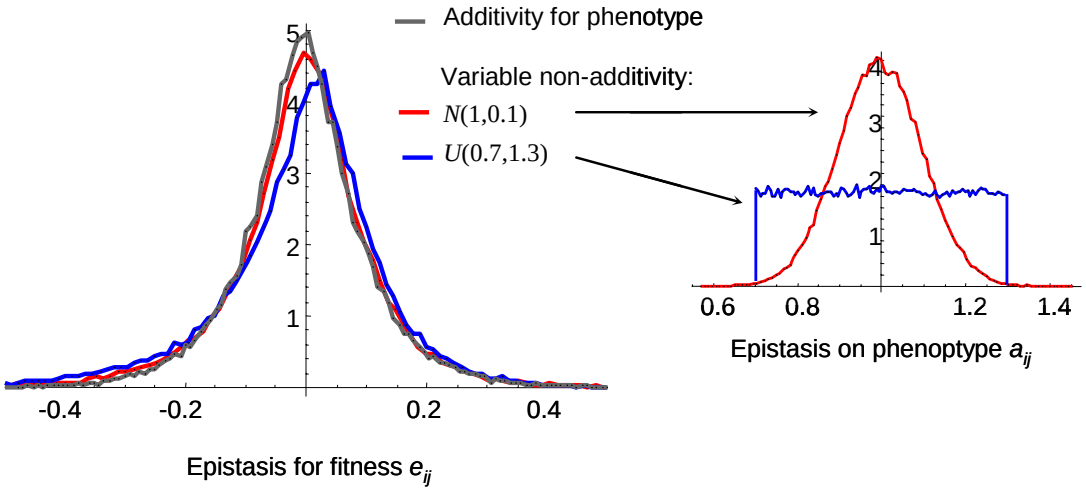

The distribution of fitness epistasis, $e_{ij} = \log(w_{ij}) - \log(w_i\ w_j)$, is simulated as in **Supplementary Figure 1.a)**, with $n_e = 3$. Simulated distributions are shown for three cases: purely additive effects of mutations on phenotype such that $\mathbf{dz}_{ij} = \mathbf{dz}_i + \mathbf{dz}_j$, or random non-additive interaction between mutations, such that $\mathbf{dz}_{ij} = a_{ij}\ (\mathbf{dz}_i + \mathbf{dz}_j)$, where a_{ij} is randomly drawn into either a Gaussian or a uniform distribution, which probability densities are given on the figure (right panel).

As long as the distribution of a_{ij} is not too variable or biased, the resulting distribution of e_{ij} (epistasis for fitness) is little affected by non-additivity between the phenotypic effects of mutations.

Supplementary Figure 3: Power curves for the tests shown in Table 1.

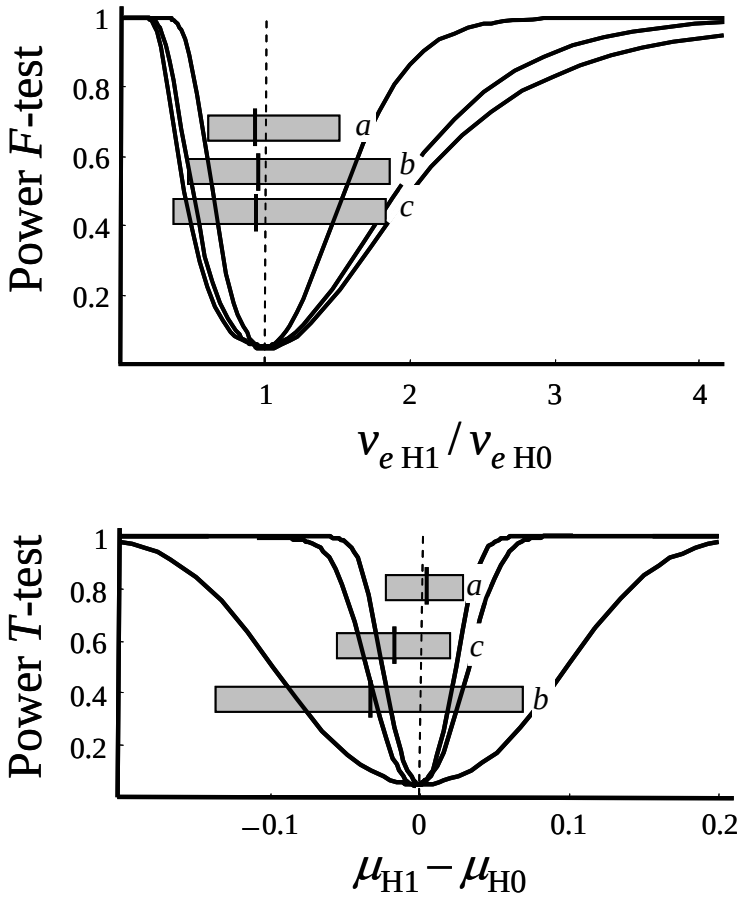

The lines correspond to the power curves of the tests given in **Table 1** for different alternative hypotheses H1, regarding the ratio of variance for *F*-test or the difference of means for *t*-tests (*x*-axis). (*a*) Tests on VSV for all mutations; (*b*) tests on *E.coli*, and (*c*) tests for VSV beneficial mutations. Note that we used a χ^2 test in the latter case for comparing variances, but this is similar to an *F*-test with an infinite number of degree of freedom on the denominator, so that we report it on the same figure. The grey bar shows the point estimate in each case and its 95% confidence interval (either $v_{e\,obs}/v_{e\,pred}$ or $\mu_{e\,obs} - \mu_{e\,pred}$). The dashed lines correspond to our prediction.